Taylor & Francis
Taylor & Francis Group

Combustion Theory and Modelling

ISSN: 1364-7830 (Print) 1741-3559 (Online) Journal homepage: http://www.tandfonline.com/loi/tctm20

Effects of endothermic chain-branching reaction on spherical flame initiation and propagation

Haiyue Li, Huangwei Zhang & Zheng Chen

To cite this article: Haiyue Li, Huangwei Zhang & Zheng Chen (2018): Effects of endothermic chain-branching reaction on spherical flame initiation and propagation, Combustion Theory and Modelling, DOI: 10.1080/13647830.2018.1555338

To link to this article: https://doi.org/10.1080/13647830.2018.1555338

Published online: 09 Dec 2018.

Combustion Theory and Modelling, 2018
https://doi.org/10.1080/13647830.2018.1555338

Effects of endothermic chain-branching reaction on spherical flame initiation and propagation

Haiyue Li[a], Huangwei Zhang[b] and Zheng Chen [a,c*]

[a]*CCSE, CAPT, SKLTCS, College of Engineering, Peking University, Beijing, People's Republic of China;* [b]*Department of Mechanical Engineering, National University of Singapore, Singapore, Singapore;* [c]*Beijing Innovation Center for Engineering Science and Advanced Technology, Peking University, Beijing, People's Republic of China*

(*Received 24 January 2018; accepted 27 November 2018*)

A theoretical model is developed to describe the spherical flame initiation and propagation. It considers endothermic chain-branching reaction and exothermic recombination reaction. Based on this model, the effects of endothermic chain-branching reaction on spherical flame initiation and propagation are assessed. First, the analytical solutions for the distributions of fuel and radical mass fraction as well as temperature are obtained within the framework of large activation energy and quasi-steady assumption. Then, a correlation describing spherical flame initiation and propagation is derived. Based on this correlation, different factors affecting spherical flame propagation and initiation are examined. It is found that endothermicity of the chain-branching reaction suppresses radical accumulation at the flame front and thus reduces flame intensity. With the increase of endothermicity, the unstretched flame speed decreases while both flame ball radius and Markstein length increases. Endothermicity has a stronger effect on the stretched flame speed with larger fuel Lewis number. The Markstein length is found to increase monotonically with endothermicity. Furthermore, the endothermicity of the chain-branching reaction is shown to affect the transition among different flame regimes including ignition kernel, flame ball, propagating spherical flame, and planar flame. The critical ignition power radius increases with endothermicity, indicating that endothermicity inhibits the ignition process. The influence of endothermicity on ignition becomes relatively stronger at higher crossover temperature or higher fuel Lewis number. Moreover, one-dimensional transient simulations are conducted to validate the theoretical results. It is shown that the quasi-steady-state assumption used in theoretical analysis is reasonable and that the same conclusion on the effects of endothermic chain-branching reaction can be drawn from simulation and theoretical analysis.

Keywords: ignition; spherical flame propagation; endothermic reaction; Lewis number

1. Introduction

Due to its simple one-dimensional configuration, spherical flame has been popularly used in theoretical studies on ignition and premixed flame propagation. One-step, irreversible, global reaction model is usually used in theoretical analysis of spherical flame (e.g. [1–6]). In the one-step chemistry model, fuel is converted directly into products and heat, and thereby the combustion is mainly controlled by fuel and heat transport. However,

*Corresponding author. Email: cz@pku.edu.cn

during the combustion process of hydrocarbon fuels in practical engines, the fuel oxidation involves numerous elementary reactions and intermediate species. As such, ignition and flame propagation are affected not only by transport of fuel and heat but also by the transport and chemical properties of intermediate species (especially radicals involved in chain-branching reactions) [7].

In order to consider the role of intermediate species, two-step chemistry model rather than one-step model should be used in theoretical analysis. Recently, the two-step chain-branching model proposed by Dold and coworkers [7–9] has been popularly used in the theoretical analysis of premixed combustion. This model is the simplified version of Zel'dovich-Liñán model [10,11]. It comprises a chain-branching reaction and a recombination reaction. This two-step chain-branching model was used in previous studies on the ignition, propagation, extinction, and stability of premixed flames. For examples, Zhang et al. [12–14] studied the effects of radical transport on critical ignition conditions and stretched flame propagation; Bai et al. [15] and Zhang et al. [16] examined the effects of radical quenching on the extinction of premixed flame; Gubernov et al. [17–20] and Sharpe et al. [21,22] investigated the instability of premixed flames. More recently, Gubernov et al. [23] proposed a chain-reaction model which can be used to describe both premixed and diffusion flames. In these studies [7–9,12,13,15–18,21,22], the chain-branching reaction is assumed to be thermally neutral and thereby the completion reaction releases all the heat. However, in practical combustion of hydrocarbon fuels, the chain-branching reaction is usually endothermic rather than thermally neutral [7]. Currently, it is not clear how the endothermicity of the chain-branching reaction affects premixed flame initiation and propagation. This motivates the present work, which aims to answer this question.

In fact, the influence of endothermic reaction on premixed flame propagation has been studied based on parallel or sequential two-step chemistry model without considering intermediate species. For example, using the paralleled exothermic and endothermic reaction model, Simon et al. [24], Gray et al. [25], and Lazarovici et al. [26] found that the endothermic reaction can quench the flame under certain conditions. Gubernov et al. [27,28] conducted stability analysis and found that the competitive endothermic reaction can lead to different flame regimes. Please et al. [29] and Qian et al. [30] studied combustion waves with sequential endothermic and exothermic chemical model and observed similar quenching effects due to the endothermic reaction. These studies indicate that endothermic reaction may have a strong impact on premixed flames. However, ignition and endothermic chain-branching reaction were not investigated before. Therefore, the present work focuses on ignition and spherical flame propagation with endothermic chain-branching reaction.

Due to its simple geometry, propagating spherical flames are popularly used to measure the laminar flame speed of different fuel/air mixtures. Experimentally, static homogeneous combustible mixture in a closed chamber is centrally ignited by an electrical spark or a laser beam which results in an outwardly propagating spherical flame. The flame front history and/or the pressure rise history are/is recorded during the experiment and used to obtain the laminar flame speed. As reviewed in [31–33], there are more than 30 groups which conduct spherical flame experiments. In addition, such experiments were also used to study the ignition process and minimum ignition energy (e.g. [34,35]). However, it is difficult to assess of the effects of endothermic chain-branching reaction on spherical flame initiation and propagation. Therefore, theoretical analysis with simplified chemical model is conducted there.

The objective of this work is to assess the effects of endothermicity of chain-branching reaction on spherical flame initiation and propagation. The two-step reaction model

containing endothermic chain-branching reaction and exothermic recombination reaction is used. Unlike previous studies [7–9,12,13,15–18,21,22], the endothermicity of the chain-branching reaction is considered for the first time. First, the analytical solutions for spherical flame initiation and propagation are obtained within the framework of large activation energy and quasi-steady assumptions. Then, the effects of endothermic chain-branching reaction on flame propagation speed, Markstein length, ignition kernel development, and critical ignition conditions are examined.

2. Mathematical model

We use the following two-step chain-branching model proposed by Dold and coworkers [7–9]:

$$F + Z \rightarrow 2Z: \quad \tilde{k}_B = \tilde{A}_B \exp(-\tilde{T}_B/\tilde{T}), \tag{1a}$$

$$Z + M \rightarrow P + M: \tilde{k}_C = \tilde{A}_C, \tag{1b}$$

where F, Z, P, and M denote fuel, radical, product, and the third body, respectively. $\tilde{A}_B$, $\tilde{A}_C$, and $\tilde{T}_B$ are the frequency factor and activation temperature. The above model involves a thermally-sensitive chain-branching reaction (1a) with a rate constant $\tilde{k}_B$ in the Arrhenius form and a completion reaction (1b) with a rate constant $\tilde{k}_C$, which is independent of temperature $\tilde{T}$.

Spherical flame initiation and propagation are studied by the classical reactive-diffusive model, in which density $\tilde{\rho}$, specific heat $\tilde{C}_P$, diffusion coefficients of fuel $\tilde{D}_F$ and radical $\tilde{D}_Z$, thermal conductivity $\tilde{\lambda}$, and global heat release $\tilde{Q}$ are assumed to be constant [36,37]. The one-dimensional conservation equations for temperature, $\tilde{T}$, and mass concentrations of fuel, $\tilde{Y}_F$, and radical, $\tilde{Y}_Z$, in a spherical coordinate are

$$\tilde{\rho}\frac{\partial \tilde{Y}_F}{\partial \tilde{t}} = \frac{1}{\tilde{r}^2}\frac{\partial}{\partial \tilde{r}}(\tilde{r}^2\tilde{\rho}\tilde{D}_F\frac{\partial \tilde{Y}_F}{\partial \tilde{r}}) - \tilde{W}_F\tilde{\omega}_B, \tag{2a}$$

$$\tilde{\rho}\frac{\partial \tilde{Y}_Z}{\partial \tilde{t}} = \frac{1}{\tilde{r}^2}\frac{\partial}{\partial \tilde{r}}(\tilde{r}^2\tilde{\rho}\tilde{D}_Z\frac{\partial \tilde{Y}_Z}{\partial \tilde{r}}) + \tilde{W}_Z(\tilde{\omega}_B - \tilde{\omega}_C), \tag{2b}$$

$$\tilde{\rho}\tilde{C}_P\frac{\partial \tilde{T}}{\partial \tilde{t}} = \frac{1}{\tilde{r}^2}\frac{\partial}{\partial \tilde{r}}(\tilde{r}^2\tilde{\lambda}\frac{\partial \tilde{T}}{\partial \tilde{r}}) + \tilde{Q}_C\tilde{\omega}_C - \tilde{Q}_B\tilde{\omega}_B, \tag{2c}$$

where $\tilde{t}$ and $\tilde{r}$ are time and radial coordinate, respectively. According to the constant-density assumption, thermal expansion is neglected and thereby the convective flux is zero. $\tilde{Q}_C$ is the heat release of completion reaction and $\tilde{Q}_B$ is the endothermicity of the chain-branching reaction. Therefore the global heat release, $\tilde{Q}$, equals the difference between them. The reaction rates are:

$$\tilde{\omega}_B = \frac{\tilde{\rho}\tilde{Y}_F}{\tilde{W}_F}\frac{\tilde{\rho}\tilde{Y}_Z}{\tilde{W}_Z}\tilde{A}_B\exp(-\frac{\tilde{T}_B}{\tilde{T}}),\ \tilde{\omega}_C = \frac{\tilde{\rho}\tilde{Y}_Z}{\tilde{W}_Z}\frac{\tilde{\rho}}{\tilde{W}}\tilde{A}_C, \tag{3}$$

where $\tilde{W}_F$ and $\tilde{W}_Z$ are molecular weights of fuel and radical, respectively, and $\tilde{W}$ represents the mean molecular weight.

Following Sharpe [21], we introduce the following non-dimensional variables:

$$r=\frac{\tilde{r}}{\tilde{\delta}}, u=\frac{\tilde{u}}{\tilde{S}_u^0}, Y_F=\frac{\tilde{Y}_F}{\tilde{Y}_{F0}}, Y_Z=\frac{\tilde{Y}_Z\tilde{W}_F}{\tilde{Y}_{F0}\tilde{W}_Z}, T=\frac{\tilde{T}}{\tilde{T}_0}, \quad Q_B=\frac{\tilde{Q}_B\tilde{Y}_{F0}}{\tilde{W}_F\tilde{C}_P\tilde{T}_0} \quad , \quad Q_C=\frac{\tilde{Q}_C\tilde{Y}_{F0}}{\tilde{W}_F\tilde{C}_P\tilde{T}_0} \quad , \tag{4}$$

where $\tilde{Y}_{F0}$ is the fuel mass fraction in the unburned mixture and $\tilde{T}_0$ is the room temperature. The characteristic speed $\tilde{S}_u^0$ and characteristic length $\delta=\tilde{\lambda}/(\tilde{\rho}\tilde{C}_P\tilde{S}_u^0)$ are the laminar flame speed and flame thickness of an adiabatic planar flame with an initial temperature of $\tilde{T}_0=$ 298K.

In the coordinates attached to the propagating spherical flame front, the non-dimensional governing equations for temperature, T, and mass fractions of fuel, Y_F, and radical, Y_Z, in the unburned and burned zones are [12,38].

$$\frac{\partial Y_F}{\partial t}-U\frac{\partial Y_F}{\partial r}=\frac{1}{Le_F}\frac{1}{r^2}\frac{\partial}{\partial r}(r^2\frac{\partial Y_F}{\partial r})-\omega, \tag{5a}$$

$$\frac{\partial Y_Z}{\partial t}-U\frac{\partial Y_Z}{\partial r}=\frac{1}{Le_Z}\frac{1}{r^2}\frac{\partial}{\partial r}(r^2\frac{\partial Y_Z}{\partial r})+\omega-\Lambda Y_Z, \tag{5b}$$

$$\frac{\partial T}{\partial t}-U\frac{\partial T}{\partial r}=\frac{1}{r^2}\frac{\partial}{\partial r}(r^2\frac{\partial T}{\partial r})-Q_B\omega+Q_C\Lambda Y_Z, \tag{5c}$$

where $Le_F=\tilde{\lambda}/(\tilde{\rho}\tilde{C}_P\tilde{D}_F)$ and $Le_Z=\tilde{\lambda}/(\tilde{\rho}\tilde{C}_P\tilde{D}_Z)$ are the Lewis numbers of the fuel and radical, respectively. $U=\mathrm{d}R(t)/\mathrm{d}t$ is propagation speed of the flame front. Q_B and Q_C are the specific heat release of the completion reaction.

In Equations 5(a)–(c), the non-dimensional branching reaction rate is [15]

$$\omega=\Lambda\Theta^2Y_FY_Z\exp\left[T_B\left(\frac{1}{T_C}-\frac{1}{T}\right)\right], \tag{6}$$

where $T_B=\tilde{T}_B/\tilde{T}_0$ and $T_C=\tilde{T}_C/\tilde{T}_0$ are the non-dimensional activation temperature and in-homogeneous chain-branching crossover temperature, respectively [7], and $\Theta=T_B/T_C$. The non-dimensional rate constant, $\Lambda=\tilde{\lambda}\tilde{A}_C/\tilde{C}_P(\tilde{S}_u^0)^2\tilde{W}$, is given implicitly by [21]:

$$\Lambda Le_Z=\left(1+\frac{1-T_C}{Q}\right)(S_2^2-S_2)(S_1-S_2), \quad S_{1,2}=\frac{Le_Z\pm\sqrt{{Le_Z}^2+4\Lambda Le_Z}}{2}. \tag{7}$$

In this study, the impact of external energy deposition on spherical flame initiation and propagation is investigated and the ignition energy is provided as a heat flux at the centre. Steady-state energy deposition is employed in order to achieve an analytical solution and the boundary conditions are [39],

$$r\to 0: \quad r^2\frac{\partial T}{\partial r}=-q\,, \frac{\partial Y_F}{\partial r}=0, \frac{\partial Y_Z}{\partial r}=0, \tag{8a}$$

$$r\to\infty: \quad T=1, \quad Y_F=1, \quad Y_Z=0, \tag{8b}$$

where q is the ignition power normalised by $4\pi\tilde{\lambda}\tilde{\delta}\tilde{T}_0$.

3. Theoretical analysis

The flame propagation is assumed to be in a quasi-steady state in the coordinate attached to the propagating flame front. This quasi-steady assumption was validated and used in previous studies (e.g. [1–3,6,12]). Moreover, in the asymptotic limit of large activation energy ($T_B \to +\infty$), the chain-branching reaction is confined at an infinitesimally thin flame sheet ($r = R$). At the two sides (i.e. the unburned and burned zones) of the flame sheet, we have $\omega = 0$. Based on these assumptions, the governing equations in Equations 5(a)–(c) are reduced to:

$$-U\frac{\mathrm{d}Y_F}{\mathrm{d}r} = \frac{1}{Le_F}\frac{1}{r^2}\frac{\mathrm{d}}{\mathrm{d}r}\left(r^2\frac{\mathrm{d}Y_F}{\mathrm{d}r}\right), \tag{9a}$$

$$-U\frac{\mathrm{d}Y_Z}{\mathrm{d}r} = \frac{1}{Le_Z}\frac{1}{r^2}\frac{\mathrm{d}}{\mathrm{d}r}\left(r^2\frac{\mathrm{d}Y_Z}{\mathrm{d}r}\right) - \Lambda Y_Z, \tag{9b}$$

$$-U\frac{\mathrm{d}T}{\mathrm{d}r} = \frac{1}{r^2}\frac{\mathrm{d}}{\mathrm{d}r}\left(r^2\frac{\mathrm{d}T}{\mathrm{d}r}\right) + Q_C\Lambda Y_Z. \tag{9c}$$

According to the asymptotic analysis conducted by Dold [7], the following conditions must hold across or at the flame front:

$$\begin{aligned}[Y_F] = [Y_Z] = [T] = \left[\frac{1}{Le_F}\frac{\mathrm{d}Y_F}{\mathrm{d}r} + \frac{1}{Le_Z}\frac{\mathrm{d}Y_Z}{\mathrm{d}r}\right] = T - T_C \\ = Y_F\frac{\mathrm{d}T}{\mathrm{d}r} = [\frac{\mathrm{d}T}{\mathrm{d}r}] - \frac{Q_B}{Le_F}[\frac{\mathrm{d}Y_F}{\mathrm{d}r}] = 0,\end{aligned} \tag{10}$$

where $[f] = f(r = \mathrm{R}+) - f(r = \mathrm{R}-)$. It is noted that here Q_B denotes the non-dimensional endothermicity of the chain-branching reaction. The global heat release is $Q = Q_C$–Q_B. Equation 9(a)–(c) can be solved analytically in the unburned and burned zones respectively. The exact solutions for fuel mass fraction, radical mass fraction and temperature are:

$$Y_F(r) = \begin{cases} 0 & \text{if } 0 \le r \le R \\ 1 - \dfrac{\int_r^\infty \xi^{-2}e^{-Le_F U\xi}\mathrm{d}\xi}{\int_R^\infty \xi^{-2}e^{-Le_F U\xi}\mathrm{d}\xi} & \text{if } r \ge R \end{cases}, \tag{11}$$

$$Y_Z(r) = \begin{cases} Y_{Zf}\exp[0.5(ULe_Z + k)(R - r)]\dfrac{F(kr, ULe_Z/k, -ULe_Z/k)}{F(kR, ULe_Z/k, -ULe_Z/k)} & \text{if } 0 \le r \le R \\ Y_{Zf}\exp[0.5(ULe_Z + k)(R - r)]\dfrac{G(-kr, ULe_Z/k, -ULe_Z/k)}{G(-kR, ULe_Z/k, -ULe_Z/k)} & \text{if } r \ge R \end{cases}, \tag{12}$$

$$T(r) = \begin{cases} T_C + \int_r^R\int_0^s I(s,\xi)\mathrm{d}\xi\,\mathrm{d}s + q\int_r^R s^{-2}e^{-Us}\mathrm{d}s & \text{if } 0 \le r \le R \\ [T_C + \int_R^\infty\int_s^\infty I(s,\xi)\mathrm{d}\xi\,\mathrm{d}s]\dfrac{\int_r^\infty s^{-2}e^{-Us}\mathrm{d}s}{\int_R^\infty s^{-2}e^{-Us}\mathrm{d}s} - \int_r^\infty\int_s^\infty I(s,\xi)\mathrm{d}\xi\,\mathrm{d}s & \text{if } r \ge R \end{cases}, \tag{13}$$

where

$$F(a,b,c)=\int_0^1 e^{at}t^b(1-t)^c\mathrm{d}t, G(a,b,c)=\int_0^\infty e^{at}t^b(1+t)^c\mathrm{d}t,$$

$$k=\sqrt{(ULe_Z)^2+4\Lambda Le_Z},$$

$$Y_{Zf}=\frac{Le_ZLe_F{}^{-1}k^{-1}R^{-2}e^{-Le_FUR}/\int_R^\infty \xi^{-2}e^{-Le_FU\xi}\mathrm{d}\xi}{\dfrac{F(kR,1+ULe_Z/k,-ULe_Z/k)}{F(kR,ULe_Z/k,-ULe_Z/k)}+\dfrac{G(-kR,1+ULe_Z/k,-ULe_Z/k)}{G(-kR,ULe_Z/k,-ULe_Z/k)}}, \quad (14)$$

$$I(s,\xi)=(\frac{\xi}{s})^2e^{-U(s-\xi)}Q_C\Lambda Y_Z(\xi).$$

Substituting the temperature distribution into the jump conditions in Equation (10), we obtain the following correlation depicting the change of the flame propagation speed U with flame radius R:

$$\int_R^\infty\int_0^s I(s,\xi)\mathrm{d}\xi\mathrm{d}s+q\int_R^\infty s^{-2}e^{-Us}\mathrm{d}s - \frac{Q_B}{Le_F}e^{UR(1-Le_F)}\frac{\int_R^\infty s^{-2}e^{-Us}\mathrm{d}s}{\int_R^\infty s^{-2}e^{-Le_FUs}\mathrm{d}s}=T_C-1. \quad (15)$$

The difference between present correlation, Equation (15) and that in previous work [12] is the term which is proportional to the endothermicity Q_B. Consequently, it can be reduced to previous solutions for flame balls, propagating spherical flames and planar flames in limiting cases. Therefore, Equation (15) is a general solution to describe adiabatic flame balls, propagating spherical flames, and planar flames with endothermic chain-branching reaction. As will be shown later, the dynamics of flame kernel growth and the transition among different flame regimes can be predicted by this correlation. Based on Equation (15), spherical flame propagation and initiation will be investigated and the effects of endothermic chain-branching reaction will be examined by changing the value of Q_B in the following section.

4. Results and discussion

To assess the effects of endothermicity of chain-branching reaction on spherical flame propagation and ignition, we change the value of non-dimensional endothermicity Q_B while fix the global heat release $Q=6$ (i.e. the adiabatic flame temperature is around 2100 K, $Q=Q_C$–Q_B). Typical values of non-dimensional parameters of $Le_F=Le_Z=1$ and $T_C=4$ (the corresponding dimensional temperature is around 12,002 K) are used unless otherwise specified. These are typical values also discussed and used by Dold [7].

4.1. *Effects of endothermicity on spherical flame propagation*

We first study the spherical flame propagation without ignition power deposition at the centre (i.e. $q=0$ in Equation (15)). Figure 1 shows the effects of endothermicity of chain-branching reaction on spherical flame propagation speed at different values of fuel Lewis number. Solutions on the horizontal axis with $U=0$ are for flame balls and those on the

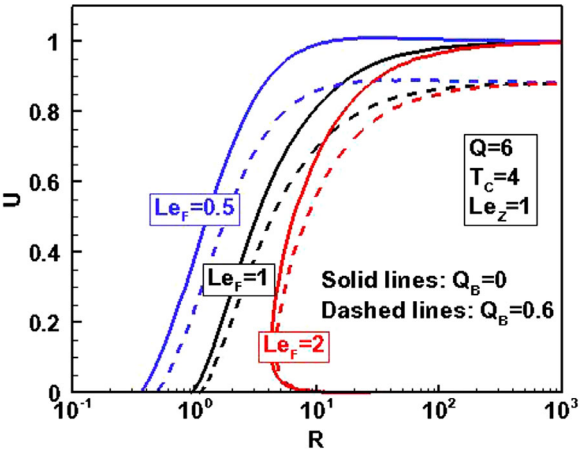

Figure 1. Spherical flame propagation speed as a function of flame radius.

right vertical axis with $R = +\infty$ are for planar flames, while the region between these two limits represents propagating spherical flame. The effects of endothermic reaction on these three types of flames will be separately discussed later. It is observed that flame propagation speed reduces when the endothermicity of chain-branching reaction is increased from $Q_B = 0$ to $Q_B = 0.6$. Therefore, the endothermicity of chain-branching reaction weakens the premixed flame propagation. This is consistent with previous results based on parallel or sequential two-step chemistry model [25–30].

The effects of endothermic reaction on unstretched planar flames are analysed first. Figure 2 shows the effects of endothermicity of chain-branching reaction on the planar flame structure. The renormalised temperature is defined as $\theta = (T - 1)/Q$. It is observed that endothermicity slightly suppresses the radical accumulation and thus reduces flame intensity. Consequently, the flame speed decreases as the endothermicity increases. This trend is demonstrated in Figure 3.

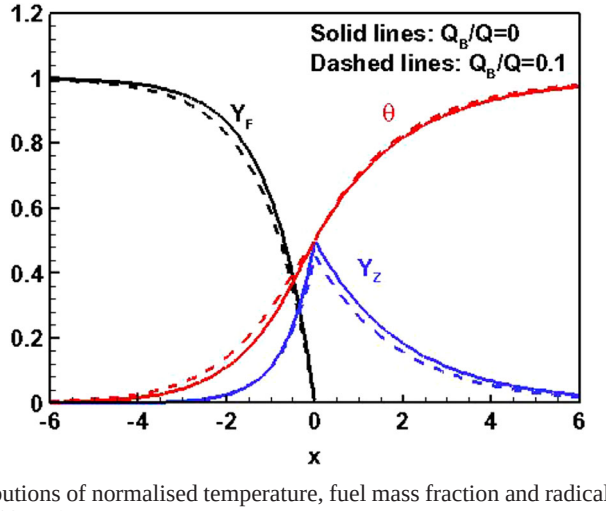

Figure 2. Distributions of normalised temperature, fuel mass fraction and radical mass fraction for $Q_B/Q = 0$ and $Q_B/Q = 0.1$.

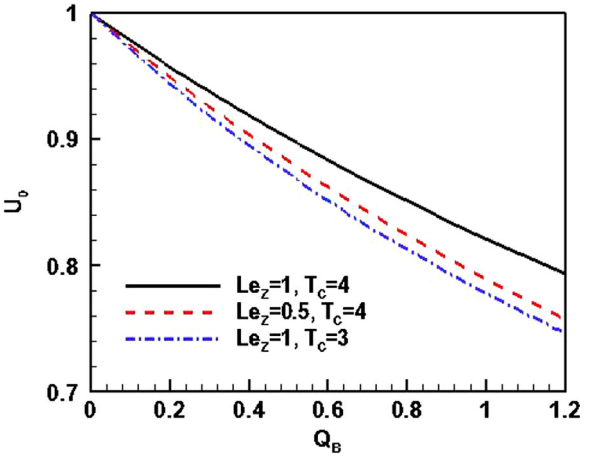

Figure 3. Change of planar flame speed with endothermicity.

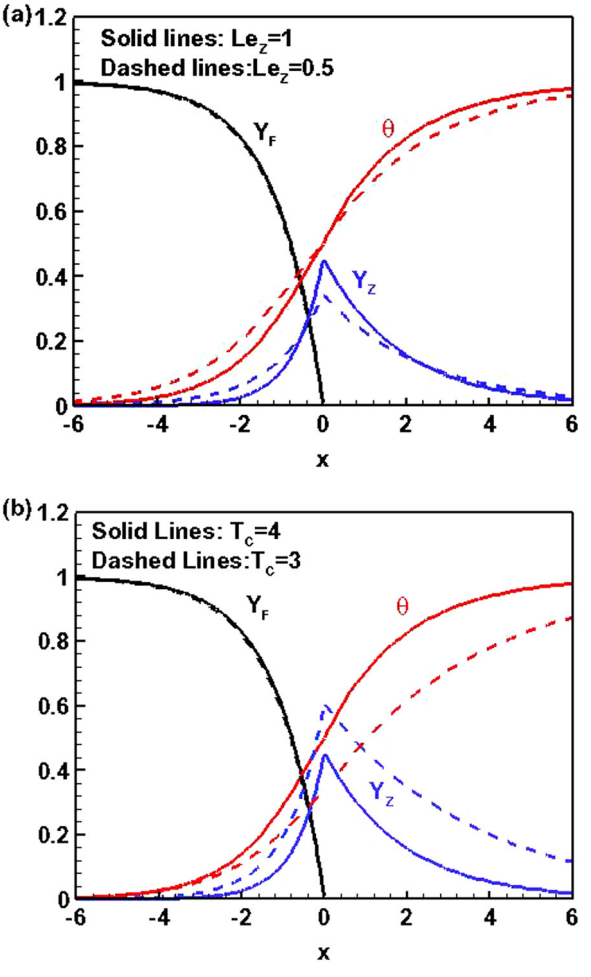

Figure 4. Effects of (a) radical Lewis number and (b) crossover temperature on planar flame structure for $Q_B/Q = 0.1$ and $Le_F = 1.0$.

Figure 3 shows that the influence of endothermicity becomes stronger at lower radical Lewis number or lower crossover temperature. This can be explained by the planar flame structure shown in Figure 4. Since lower radical Lewis number corresponds to higher mass diffusivity of radical, the radical concentration at the flame front is smaller for lower Le_Z. Consequently, at lower Le_Z, the flame becomes weaker and is more strongly affected by endothermicity of chain-branching reaction. At lower crossover temperature T_C, the chain-branching reaction becomes faster and the radical concentration becomes larger as shown in Figure 4(b). Meanwhile, the influence of endothermicity becomes stronger since it is also proportional to the reaction rate of the chain-branching reaction in the governing equation for temperature, Equation 9(c).

Figure 1 shows that similar to the planar flame, the positively stretched spherical flame has lower propagation speed as the endothermicity of chain-branching reaction is considered. Figure 5 shows the change of spherical flame propagation speed with the stretch rate, which is $K = 2U/R$ for spherical flame propagation. It is observed that U changes linearly with K at the low stretch rate. Therefore, the unstretched planar flame speed, U_0 (as shown in Figure 3), and Markstein length, L, can be obtained from linear extrapolation. The Markstein length characterises the sensitivity of flame propagation speed to stretch rate. As expected, the influence of stretch on flame speed becomes stronger at higher fuel Lewis number. Moreover, Figure 5 shows that the effects of endothermicity become stronger at the larger stretch rate. Therefore, compared to an unstretched planar flame, stretched flame is more easily affected by the endothermic reaction. The Markstein length represents the sensitivity of flame speed to stretch rate. The influence of endothermicity of chain-branching reaction on Markstein length is shown in Figure 6. It is seen that the Markstein length L increases monotonically with the endothermicity Q_B. This is because the flame becomes weaker when the chain-branching reaction becomes endothermic and weaker flame is more sensitive to stretch rate [40]. The influence of endothermicity is similar to that of radiative loss [38,41] and droplet evaporation [42] which also weaken the flame and increase the Markstein length.

In the next subsection, ignition of spherical flame will be investigated. It is well-known that the critical ignition condition greatly depends on the flame ball radius. Therefore, we also examine the influence of the endothermicity of chain-branching reaction on flame ball

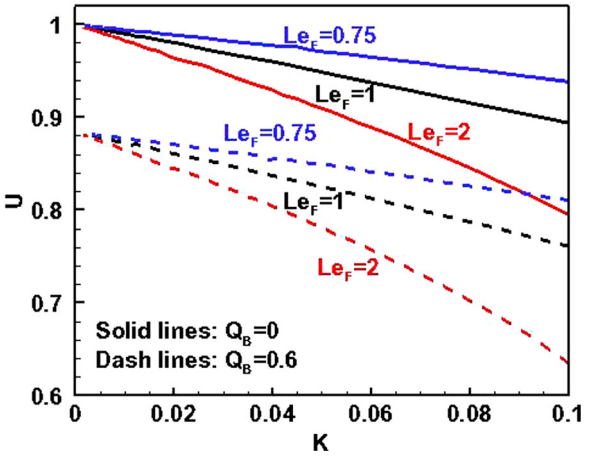

Figure 5. Spherical flame propagation speed as a function of stretch rate.

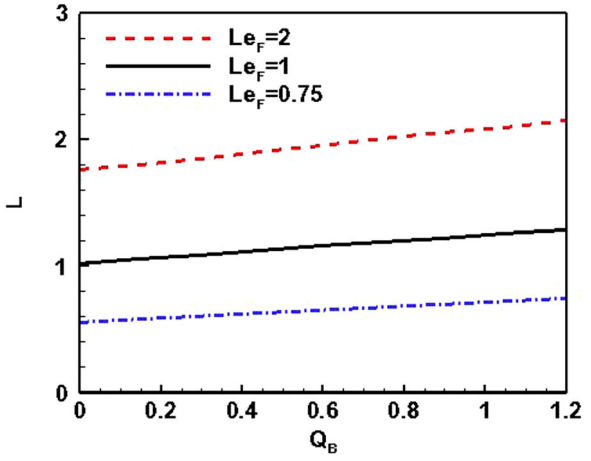

Figure 6. Change of the Markstein length with endothermicity.

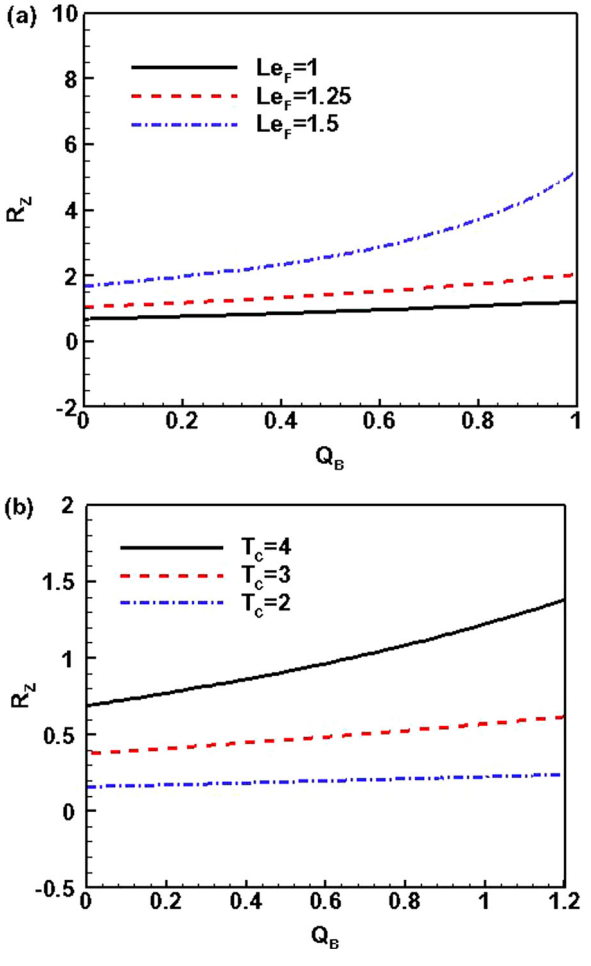

Figure 7. Change of flame ball radius with endothermicity for different values of (a) fuel Lewis number and (b) crossover temperature.

radius with zero ignition power. The results are shown in Figure 7. The flame ball radius is shown to always increase with the endothermicity. The influence of endothermicity is stronger for larger fuel Lewis number Le_F and higher crossover temperature T_C. For larger Le_F, the heat loss (due to thermal conduction away from the flame) dominates over the enthalpy gain (due to fuel diffusion into the flame) for a positively stretched spherical flame and thereby the effect of endothermicity becomes stronger. At higher T_C, less radical can be produced and the influence of endothermic reaction is stronger.

4.2. *Effects of endothermicity on spherical flame initiation*

In this subsection, we examine the effects of endothermicity of chain-branching reaction on ignition kernel development and critical ignition conditions.

To initialise the ignition kernel, an external energy flux ($q > 0$) is deposited in the centre of a quiescent pre-mixture. Figures 8 and 9 show the spherical flame propagation speed

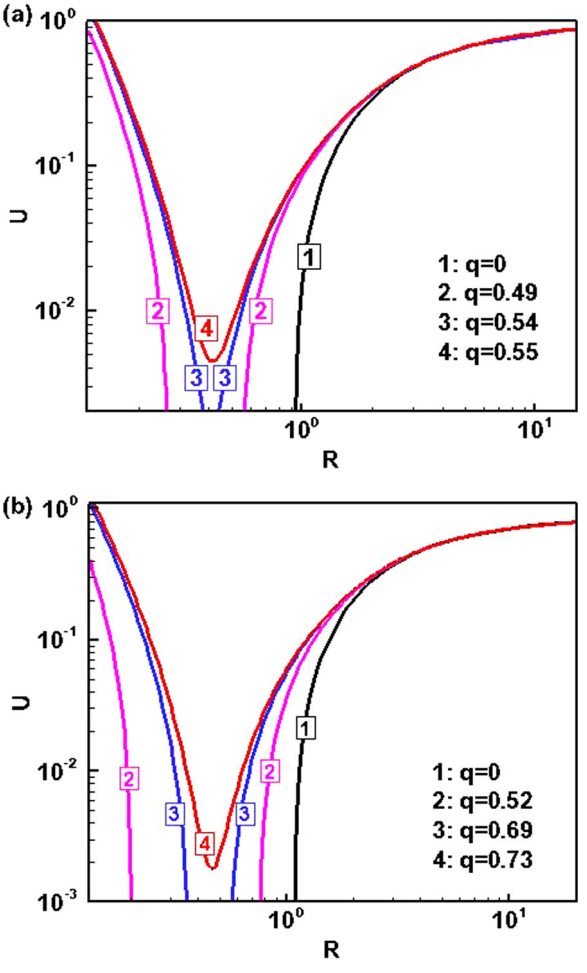

Figure 8. Flame propagation speed as a function of flame radius at different ignition powers for (a) $Q_B = 0.0$ and (b) $Q_B = 0.6$ for $Le_F = 1$.

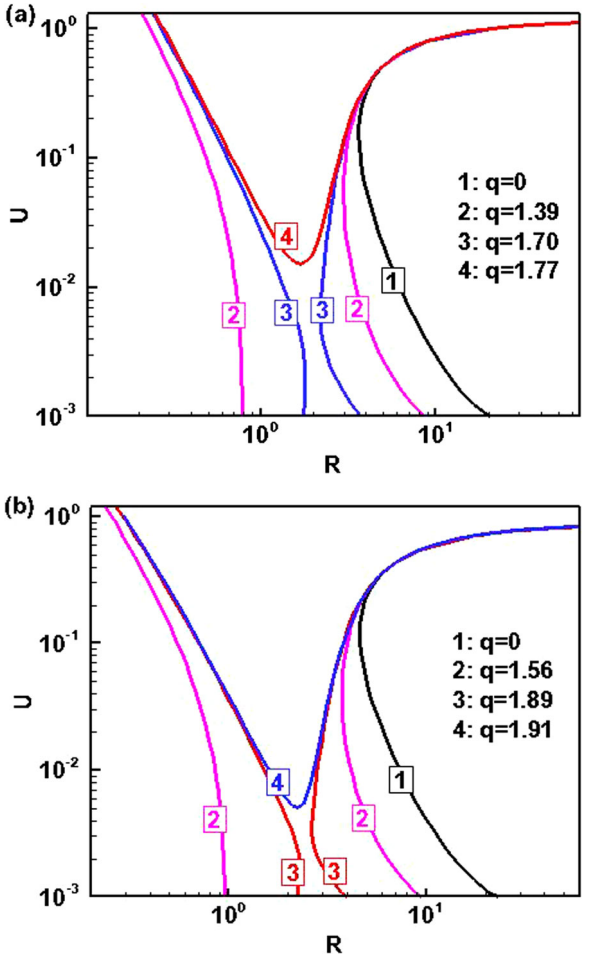

Figure 9. Flame propagation speed as a function of flame radius at different ignition powers for (a) $Q_B = 0.0$ and (b) $Q_B = 0.6$ for $Le_F = 2$.

as a function of flame radius at different ignition powers for $Le_F = 1$ and 2 respectively. For $q = 0$, the U–R curves (line #1) in Figures 8 and 9 are the same as that in Figure 1, for which the outwardly propagating spherical flame only exists beyond the flame ball solution. At low ignition powers, there exist two branches of solutions: the original travelling flame branch on the right and a new ignition kernel branch on the left. Once the external power is larger than the so-called critical (minimum) ignition power, q_c, these two branches merge resulting in a new upper branch, along which successful ignition is achieved. For $Le_F = 1$, the critical ignition power, q_c, is changed from 0.54 to 0.71 when the endothermicity of chain-branching reaction is increased from $Q_B = 0$ to $Q_B = 0.6$. However, for $Le_F = 2$, it is changed from 1.71 to 1.9 when Q_B is increased from $Q_B = 0$ to $Q_B = 0.6$.

Figure 10 shows the dependence of critical ignition power on the endothermicity of chain-branching reaction. It is seen that the critical ignition power, q_c, always increases with Q_B. Therefore, similar to radiative loss [38 41] and droplet evaporation [42], the

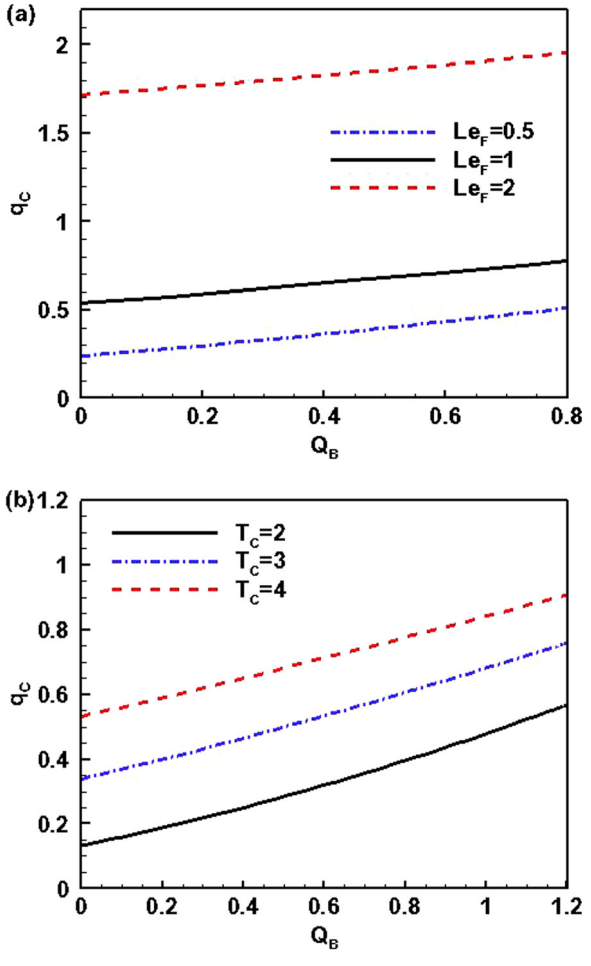

Figure 10. Change of critical ignition power with endothermicity for different values of (a) fuel Lewis number and (b) crossover temperature.

endothermicity of the chain-branching reaction inhibits the ignition process. This is expected since the flame becomes weaker and the production and consuming rate of radicals are lower as the chain-branching reaction becomes endothermic. In the case with higher fuel Lewis number Le_F, the difference between the enthalpy gain (due to fuel diffusion into the flame) and heat loss (due to thermal conduction away from the flame) for a positively stretched flame also gets larger. Relatively stronger effects of heat loss are intensified by endothermicity and thereby the slope of lines in Figure 10(a) is larger. However, since both critical ignition power and energy are much higher at large fuel Lewis number due to stronger stretch effect and lower propagation velocity, the normalised critical ignition power and radius scaled by corresponding values without endothermic reaction do not change significantly with endothermicity in Figure 11. Moreover, at lower crossover temperature T_C, flame gets more sensitive to the endothermic reaction and normalised ignition power increases more significantly as endothermicity according to Figure 11.

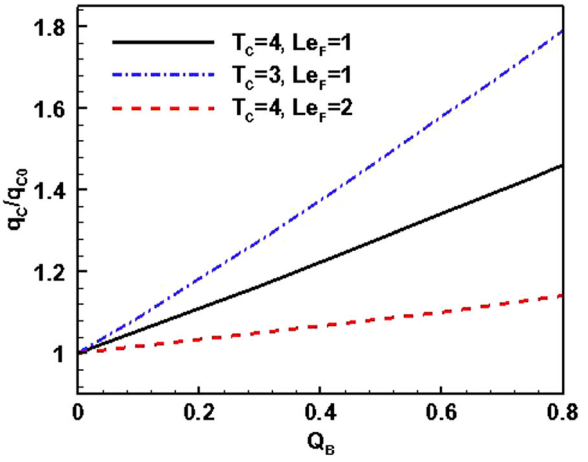

Figure 11. Normalised critical ignition power as a function of endothermicity for different values of fuel Lewis number and crossover temperature.

5. Numerical validation

In theoretical analysis, the spherical flame propagation is assumed to proceed in a quasi-steady manner and thus unsteady transition effects are neglected. Moreover, according to the large activation energy assumption, the chain-branching is restricted to an infinitely thin reaction front. To validate the theoretical analysis, we conduct transient numerical simulations with finite activation energy. The time-dependent system given by Equations 5(a)–(c) is solved by the finite volume method. The numerical methods are similar to those described in Reference [43]. The only difference is that here two-step chemistry instead of detailed chemistry is considered. In simulation, a seven-level adaptive gridding algorithm is employed to accurately and efficiently resolve the moving flame front, where the mesh addition and removal are based on the gradient and curvature of the temperature distribution. The computation domain is $0 \leq r \leq 1040$. The boundary conditions of zero gradient for temperature, fuel and radical mass fraction are used at both $r = 0$ and $r = 1040$.

We first justify the validity of the quasi-steady-state assumption by evaluating the magnitude of the unsteady term. The numerical results from transient simulation are transformed into the flame front-attached coordinate (in which theoretical analysis is conducted). In the transformed coordinate, the magnitudes of the unsteady term $(\partial T/\partial t + U\partial T/\partial r)$, convection term $(-U\partial T/\partial r)$, diffusion term $(\partial(\partial T/r^2\partial r)r^2\partial r)$, and reaction term $(Q_C Y_Z – Q_B\omega)$ of the energy equation in the flame front-attached coordinate are compared. Figure 12 shows the results for a flame at $Le_F = 1.0$, $Le_Z = 1.0$, $Q_B = 0.6$. Compared to the convection, diffusion and reaction terms, the unsteady term is shown to be much smaller and is nearly negligible. This demonstrates that the quasi-steady assumption used in theoretical analysis is reasonable.

We then validate the main theoretical results by transient simulations. Figure 13 plots the change of spherical flame propagation speed with the flame radius. It is seen that endothermicity reduces flame propagation speed and thus inhibits flame propagation. This is consistent with theoretical results shown in Figure 1.

Figure 14 shows the change of Markstein length with endothermicity predicted transient simulation. The Markstein length is shown to monotonically increase with endothermicity, which qualitatively agrees with theoretical results shown in Figure 6.

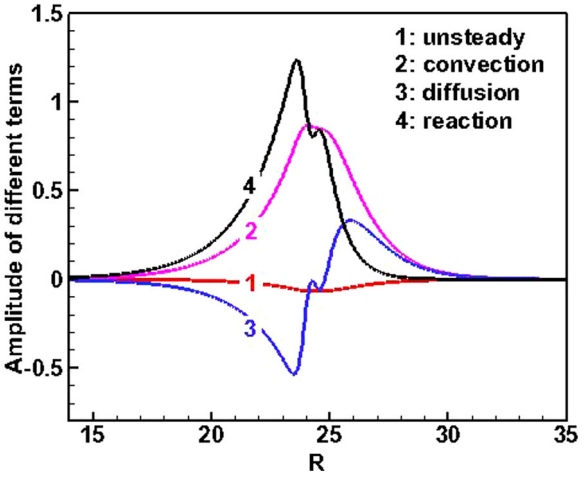

Figure 12. The unsteady term $(\partial T/\partial t + U\partial T/\partial r)$, convection term $(-U\partial T/\partial r)$, diffusion term $(\partial(\partial T/r^2\partial r)r^2\partial r)$ and reaction term $(Q_C Y_Z - Q_B\omega)$ of the energy equation in the flame front-attached coordinate for $Le_F = 1.0$, $Le_Z = 1.0$, $Q_B = 0.6$.

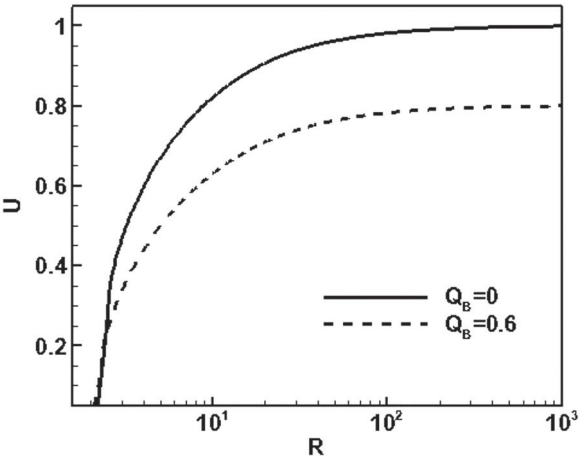

Figure 13. Change of the spherical flame propagation speed with the flame radius for $Le_F = 1.0$, $Le_Z = 1.0$.

In the simulation of spherical flame initiation, the initial temperature in the whole domain is uniformly zero. Due to the absence of chain-initiation reaction in two-step chemistry model, a small amount of radical needs to be added. Here the initial radical concentration distribution is set to be $Y_Z = 0.001e^{-5r}$, which cannot ignite the mixture without an external energy flux (i.e. $q > 0$) at the centre. A self-sustained propagation flame is shown to be successfully initiated only when the ignition energy is above the minimum ignition energy (MIE). Figure 15 shows the results for $Le_F = 2$ and $Le_Z = 1$. It is seen that for the same ignition power of $q = 1.4$, ignition succeeds when endothermicity is zero but it fails for $Q_B = 0.6$ (i.e. the endothermicity is 10% of total heat release). For $q = 1.5$, successful ignition is achieved for both $Q_B = 0$ and $Q_B = 0.6$ while endothermicity reduced the propagation speed of the spherical flame. Therefore, ignition is suppressed

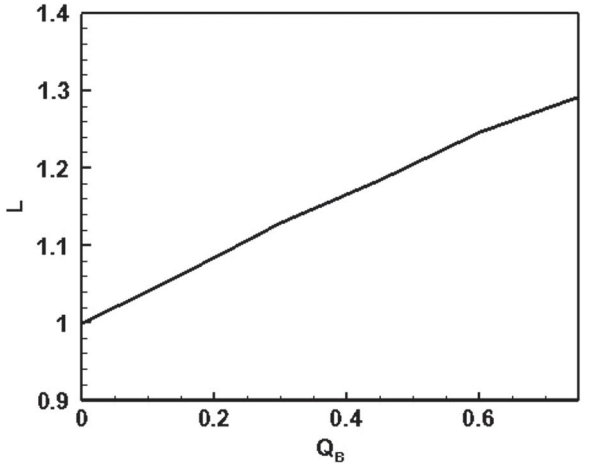

Figure 14. Change of the Markstein length with endothermicity for $Le_F = 1.0$, $Le_Z = 1.0$.

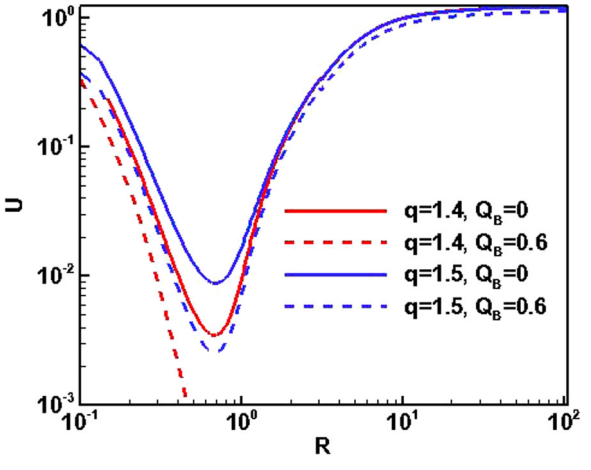

Figure 15. Flame propagation speed as a function of flame radius at different ignition powers for $Le_F = 2$ and $Le_Z = 1$.

and the MIE increases when endothermicity is included. In a brief summary, the above results in Figures 13–15 from 1D transient simulation are consistent with theoretical results from analysis based on quasi-steady assumption.

6. Conclusions

Spherical flame initiation and propagation are analysed with endothermic chain-branching reaction and exothermic recombination reaction. Within the framework of large activation energy and quasi-steady assumptions, a correlation describing spherical flame propagation speed as a function of flame radius is derived. Based on this correlation, the effects of endothermicity of chain-branching reaction on flame speed, Markstein length, ignition kernel development, and critical ignition conditions are successfully assessed. Spherical flame propagation is shown to be influenced significantly by the endothermicity of

chain-branching reaction. It is found that with the increase of endothermicity, the radical accumulation at flame front is supressed and thus the flame becomes weaker. Therefore, the flame speed decreases with the increase in endothermicity. The Markstein length is found to increase with endothermicity. Therefore, spherical flame propagation is more sensitive to the stretch rate for higher endothermicity of chain-branching reaction. Ignition is also strongly affected by the endothermicity of chain-branching reaction. The endothermicity prohibits the ignition kernel development. Therefore, the critical ignition power is found to increase with endothermicity.

It is noted that the theory is restricted to quasi-steady state and large activation energy assumptions. In order to confirm the validity of theoretical prediction, one-dimensional transient simulations with finite reaction rates are conducted. It is shown that the quasi-steady-state assumption used in theoretical analysis is reasonable and that the results from theoretical analysis agree qualitatively with those from numerical simulation.

Disclosure statement

No potential conflict of interest was reported by the authors.

Funding

HL and ZC were supported by National Natural Science Foundation of China [grant numbers 91741126 and 91541204]. HZ was supported by the start-up grant [grant number R-265-000-604-133] by the assistant professorship provided by National University of Singapore.

ORCID

Zheng Chen http://orcid.org/0000-0001-7341-6099

References

[1] M.L. Frankel and G.I. Sivashinsky, *On effects due to thermal expansion and Lewis number in spherical flame propagation*, Combust. Sci. Technol. 31 (1983), pp. 131–138.
[2] B. Deshaies and G. Joulin, *On the initiation of a spherical flame kernel*, Combust. Sci. Technol. 37 (1984), pp. 99–116.
[3] L. He, *Critical conditions for spherical flame initiation in mixtures with high Lewis numbers*, Combust. Theor. Model. 4 (2000), pp. 159–172.
[4] R. Addabbo, J.K. Bechtold, and M. Matalon, *Wrinkling of spherically expanding flames*, Proc. Combust. Inst. 29 (2002), pp. 1527–1535.
[5] C.J. Sung, A. Makino, and C.K. Law, *On stretch-affected pulsating instability in rich hydrogen/air flames: asymptotic analysis and computation*, Combust. Flame 128 (2002), pp. 422–434.
[6] Z. Chen and Y. Ju, *Theoretical analysis of the evolution from ignition kernel to flame ball and planar flame*, Combust. Theor. Model. 11 (2007), pp. 427–453.
[7] J.W. Dold, *Premixed flames modelled with thermally sensitive intermediate branching kinetics*, Combust. Theor. Model. 11 (2007), pp. 909–948.
[8] J.W. Dold, R.W. Thatcher, A. Omon-Arancibia, and J. Redman, *From one-step to chain-branching premixed flame asymptotics*, Proc. Combust. Inst. 29 (2002), pp. 1519–1526.
[9] J.W. Dold, R.O. Weber, R.W. Thatcher, and A.A. Shah, *Flame balls with thermally sensitive intermediate kinetics*, Combust. Theor. Model. 7 (2003), pp. 175–203.
[10] I.B. Zeldovich, G.I. Barenblatt, V.B. Librovich, *Mathematical Theory of Combustion and Explosions*, Consultants Bureau, New York, 1985.
[11] A. Linan, F.A. Williams, *Fundamental Aspects of Combustion*, Oxford University Press, New York, 1993.

[12] H. Zhang and Z. Chen, *Spherical flame initiation and propagation with thermally sensitive intermediate kinetics*, Combust. Flame 158 (2011), pp. 1520–1531.
[13] H. Zhang, P. Guo, and Z. Chen, *Critical condition for the ignition of reactant mixture by radical deposition*, Proc. Combust. Inst. 34 (2013), pp. 3267–3275.
[14] H. Zhang and Z. Chen, *Bifurcation and extinction limit of stretched premixed flames with chain-branching intermediate kinetics and radiative loss*, Combust. Theor. Model. 22 (2018), pp. 531–553.
[15] B. Bai, Z. Chen, H. Zhang, and S. Chen, *Flame propagation in a tube with wall quenching of radicals*, Combust. Flame 160 (2013), pp. 2810–2819.
[16] H. Zhang and Z. Chen, *Effects of heat conduction and radical quenching on premixed stagnation flame stabilised by a wall*, Combust. Theor. Model. 17 (2013), pp. 682–706.
[17] V.V. Gubernov, H.S. Sidhu, and G.N. Mercer, *Combustion waves in a model with chain branching reaction and their stability*, Combust. Theor. Model. 12 (2008), pp. 407–431.
[18] V.V. Gubernov, H.S. Sidhu, G.N. Mercer, A.V. Kolobov, and A.A. Polezhaev, *The effect of Lewis number variation on combustion waves in a model with chain-branching reaction*, J. Math. Chem. 44 (2008), pp. 816–830.
[19] V.V. Gubernov, A.V. Kolobov, A.A. Polezhaev, and H.S. Sidhu, *Stability of combustion waves in the Zeldovich–Liñán model*, Combust. Flame 159 (2012), pp. 1185–1196.
[20] V.V. Gubernov, A.V. Kolobov, A.A. Polezhaev, and H.S. Sidhu, *Analysing the stability of premixed rich hydrogen–air flame with the use of two-step models*, Combust. Flame 160 (2013), pp. 1060–1069.
[21] G.J. Sharpe, *Effect of thermal expansion on the linear stability of planar premixed flames for a simple chain-branching model: The high activation energy asymptotic limit*, Combust. Theor. Model. 12 (2008), pp. 717–738.
[22] G.J. Sharpe, *Thermal-diffusive instability of premixed flames for a simple chain-branching chemistry model with finite activation energy*, SIAM J. Appl. Math. 70 (2009), pp. 866–884.
[23] V.V. Gubernov, V.I. Babushok, and S.S. Minaev, *Phenomenological model of chain-branching premixed flames*, Combust. Theor. Model. (2018). In press. DOI:10.1080/13647830.2018.1520305.
[24] P.L. Simon, S. Kalliadasis, J.H. Merkin, and S.K. Scott, *Inhibition of flame propagation by an endothermic reaction*, IMA J Appl Math 68 (2003), pp. 537–562.
[25] B.F. Gray, S. Kalliadasis, A. Lazarovici, C. Macaskill, J.H. Merkin, and S.K. Scott, *The suppression of an exothermic branched–chain flame through endothermic reaction and radical scavenging*, Proc. Royal Soc. A: Math. Phys. Eng. Sci. 458 (2002), pp. 2119–2138.
[26] A. Lazarovici, S. Kalliadasis, J.H. Merkin, and S.K. Scott, *Flame quenching through endothermic reaction*, J. Eng. Math. 44 (2002), pp. 207–228.
[27] V.V. Gubernov, J.J. Sharples, H.S. Sidhu, A.C. McIntosh, and J. Brindley, *Properties of combustion waves in the model with competitive exo- and endothermic reactions*, J. Math. Chem. 50 (2012), pp. 2130–2140.
[28] V.V. Gubernov, S.S. Minaev, V.I. Babushok, and A.V. Kolobov, *The effect of depletion of radicals on freely propagating hydrocarbon flames*, J. Math. Chem. 53 (2015), pp. 2137–2154.
[29] C.P. Please, F. Liu, and D.L.S. McElwain, *Condensed phase combustion travelling waves with sequential exothermic or endothermic reactions*, Combust. Theor. Model 7 (2003), pp. 129–143.
[30] C. Qian, H.S. Sidhu, J.J. Sharples, I.N. Towers, and V.V. Gubernov, *Combustion waves from a sequential exothermic and endothermic reaction*, 19th International Congress on Modelling and Simulation, Perth, Australia, 2011.
[31] F.N. Egolfopoulos, N. Hansen, Y. Ju, K. Kohse-Höinghaus, C.K. Law, and F. Qi, *Advances and challenges in laminar flame experiments and implications for combustion chemistry*, Prog. Energy Combust. Sci. 43 (2014), pp. 36–67.
[32] Z. Chen, *On the accuracy of laminar flame speeds measured from outwardly propagating spherical flames: Methane/air at normal temperature and pressure*, Combust. Flame 162 (2015), pp. 2442–2453.
[33] M. Faghih and Z. Chen, *The constant-volume propagating spherical flame method for laminar flame speed measurement*, Sci. Bull. 61 (2016), pp. 1296–1310.
[34] B. Lewis, G. Von Elbe, *Combustion, Flames and Explosions of Gases*, Elsevier, New York, 2012.

[35] P.D. Ronney, *Laser versus conventional ignition of flames*, Opt. Eng. 33 (1994), pp. 510–522.
[36] G. Joulin and P. Clavin, *Linear stability analysis of nonadiabatic flames: Diffusional-thermal model*, Combust. Flame 35 (1979), pp. 139–153.
[37] P. Clavin, *Dynamic behavior of premixed flame fronts in laminar and turbulent flows*, Prog. Energy Combust. Sci. 11 (1985), pp. 1–59.
[38] H. Zhang, P. Guo, and Z. Chen, *Outwardly propagating spherical flames with thermally sensitive intermediate kinetics and radiative loss*, Combust. Sci. Technol. 185 (2013), pp. 226–248.
[39] Z. Chen, M.P. Burke, and Y. Ju, *On the critical flame radius and minimum ignition energy for spherical flame initiation*, Proc. Combust. Inst. 33 (2011), pp. 1219–1226.
[40] C.K. Law, *Combustion Physics*, Cambridge University Press, Cambridge, 2010.
[41] Z. Chen, X. Gou, and Y. Ju, *Studies on the outwardly and inwardly propagating spherical flames with radiative loss*, Combust. Sci. Technol. 182 (2010), pp. 124–142.
[42] W. Han and Z. Chen, *Effects of finite-rate droplet evaporation on the ignition and propagation of premixed spherical spray flame*, Combust. Flame 162 (2015), pp. 2128–2139.
[43] Z. Chen, *Effects of radiation and compression on propagating spherical flames of methane/air mixtures near the lean flammability limit*, Combust. Flame 157 (2010), pp. 2267–2276.